JOURNAL OF APPLIED ELECTROCHEMISTRY **26** (1996) 10–17

Production of ethene oxide in a sieve plate electrochemical reactor
Part I: Influence of sieve plate design, electrode material and pH

K. SCOTT

Department of Chemical and Process Engineering, University of Newcastle upon Tyne, NE1 7RU, Great Britain

W. HUI

British Gas plc, Loughborough, LE11 3QW Great Britain

Received 7 September 1994; revised 15 May 1995

The performance of a sieve plate electrochemical reactor for the production of ethene oxide by the indirect electrochemical oxidation of ethene is reported. The oxidant is anodically generated bromine solution. The sieve plate reactor consists of a stack of bipolar electrodes situated above a sieve plate gas distributor. Two bipolar electrode materials are used graphite and IrO_2 coated Ebonex®. The influence of different sieve plate designs on performance is described. Control of electrolyte pH is shown to be an important requirement for efficient reactor operation.

1. Introduction

The rate of electrochemical processes involving sparingly soluble organics are usually limited by the low solubility of the organic in the aqueous electrolyte. The use of a redox system assists an electrochemical process by substituting the mass transfer of the sparingly soluble organic to the electrode with the mass transfer of the redox agent to the electrodes. For the electrochemical production of alkene oxide via the bromohydrin route the electrochemical regeneration of the bromine redox catalyst can be performed *in situ*, that is, in the same reactor as the homogeneous reaction to form the ethene oxide. Figure 1 shows schematically the mechanism for the indirect electrochemical oxidation.

The overall species conservation equation is the reaction of the alkene with water

$$CH_2 = CH_2 + H_2O \longrightarrow CH_2OCH_2 + H_2 \qquad (1)$$

At the anode bromine is formed

$$2Br^- \longrightarrow Br_2 + 2e^- \qquad (2)$$

which subsequently reacts with the alkene (in this case ethene) in the solution according to the following reaction:

$$Br_2 + CH_2 = CH_2 + H_2O \longrightarrow CH_2OHCH_2Br + Br^- + H^+ \qquad (3)$$

At the cathode, the reduction of water to hydrogen gas and hydroxide ions occurs:

$$2H_2O + 2e^- \longrightarrow H_2 + 2OH^- \qquad (4)$$

The bromohydrin is transported to the alkaline cathode region where the alkene oxide is formed by the base promoted dehydrohalogenation of the vicinal bromohydrin (saponification).

$$CH_2OHCH_2Br + OH^- \longrightarrow CH_2OCH_2 + H_2O + Br^- \qquad (5)$$

Indirect electrochemical oxidation processes have found applications industrially. Some important processes are the production of anthraquinone from anthracene using Ce(IV) ions and the oxidation of glucose to gluconic acid with bromine. The electrolytic conversion of alkenes to epoxides via the bromohydrin route has been studied considerably [1–12]. The oxidation of propene has received much attention since the chlorohydrin process possesses some drawbacks and pollution problems. Table 1 summarizes cell designs investigated for ethene and propene epoxidation. The oxidations have been carried out both *in situ* and *ex situ* of the electrochemical cell. In designing an indirect electrochemical process the relative merits of both approaches needs to be considered.

A third way indirect electrolysis can occur is if the redox agent, which is activated electrochemically, is fixed at the electrode surface and is regenerated there continuously after reaction with the substrate. In this case, a separation step is unnecessary. Passivation and other problems may occur with *in situ* systems, if the organic side products or intermediates are electroactive at the applied potential.

A major factor in the epoxidation of gaseous alkenes is the low solubility in the aqueous electrolyte (approximately $5\,mol\,m^{-3}$ 1.0 bar pressure 25 °C). In

0021-891X/93

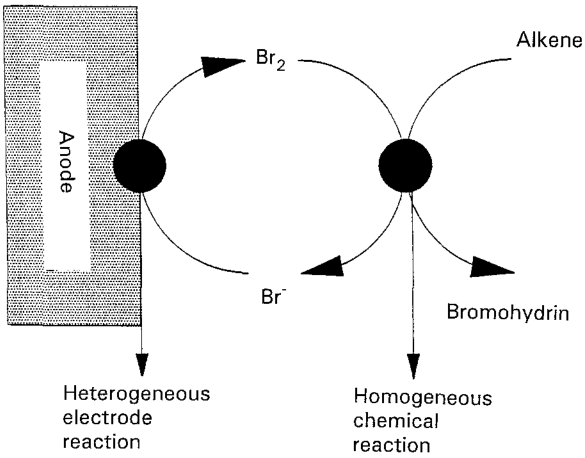

Fig. 1. Schematic view of indirect anodic oxidation of alkene.

the bromohydrin electrochemical route to alkene oxide, before the alkene can react with the electrogenerated bromine, it must first diffuse into the aqueous phase. To enhance this diffusion process, intimate contact between the alkene gas and the aqueous solution is necessary. This is often accomplished by counter currently passing the gas and liquid streams through devices having large surface area. The greater the amount of product alkene oxide required by the process (via maximizing the rate of intermediate alkene bromohydrin formation), the larger the interfacial area required. If the reaction is fast compared with the mass transfer, as in the case of the bromination of ethene, the reactor performance in the formation of the intermediate bromohydrin can be limited by its performance as a mass transfer device. The choice of a suitable gas–liquid contactor is therefore an economic problem with competition between the value of the interfacial area and the energy expense required to create it.

The cost of creating the interfacial area must therefore be compared with the cost of producing the bromine for the reaction. The ideal situation then is for all the bromine being generated to be consumed by the reaction with the alkene gas, since bromine generation constitutes a major energy requirement in the process. Any bromine remaining in solution and not reacting with the alkene gas can be considered as contributing to an energy loss, and can undergo different parasitic reactions such as the reaction to form bromate and the reduction of bromine.

Due to the low solubility of alkenes in aqueous electrolyte, the production of alkene oxide requires the use of reactor designs with good interphase mass transport. The present work on the sieve plate electrochemical reactor is an extension on the sieve plate cell design which has been previously investigated by Scoffham [7] and Harrison [8]. The latter design is based on a rectangular configuration while the reactor used in this work is based on a cylindrical absorption tower with a new weir design to minimise the influence

Table 1. Comparison of different cell designs for alkene oxide production

Cell design	*Electrolyte* /kmol m^{-3}	*Energy* /kWh kg^{-1}	*Yield* /kmol h^{-1} m^{-3}	*Current efficiency* %			*Reference*
				Alkene oxide	*Halogen byproduct*	*Glycol*	
Pullman–Kellog	NaCl	4.9	0.8	73	11	–	1
Propene Ethene	(0.1 M)	6.9	0.8	66	14	–	
Kroenig–Konrad	NaCl	3.7	1.1	89	8	0.7	9
Propene Ethene	(0.5 M)	5.2	0.9	81	10	1.0	
Simmrock	NaCl	3.8	0.13	90	7	2	10
Propene Ethene	(1.3 M)	5.1	0.08	75	22	2	
Sieve plate Cell	NaBr	2.9	0.7	92	–	–	7, 8
Propene Ethene	(0.1 M)	3.5	0.7	91	–	–	
Capillary gap	NaBr (0.2 M)	4.6	0.2	65	1.5	3	11
Pump cell	NaBr (0.2 M)						
	2000 rpm	1.6	0.05	84	–	–	2
	3000 rpm	2.7	0.10	100	–	–	
Swiss roll	NaBr (0.4 M)	2.8	–	81	5	5	3
Packed bed	NaBr (0.1 M)	21.0	0.6	100	–	–	
Bipolar rod	NaBr	3.4	0.04	77	3	–	4
	(0.5 M) 75 psi	8.6	2.7	80	2	0.5	
Trickle tower	NaBr (0.1 M)	4.5	0.1	96	–	–	5, 6

of current bypass. Data are reported for the indirect oxidation of ethene using electrogenerated bromine formed by the anodic oxidation of bromide solutions. The effect of temperature and pH on the current efficiency, selectivity and energy consumption is reported. The reactor uses either graphite or Pt/Ir coated Ebonex$^{\circledR}$ electrodes and is operated in a recycle mode. Part II of this study of the SPER [14] considers the influence of dissolved ethene concentration and current density and mathematically models the unit.

2. Experimental sieve plate electrochemical reactor

The design of the SPER reaction unit is shown in Fig. 2. The reaction unit was constructed in four sections from perspex. Section A and B comprises the main body of the bipolar electrode stack holder with section C and D allowing the attachment of different designs of sieve plate and the downcomer plate. The electrolyte enters via a pipe connection through the glassware. Section B was a Perspex box, 18 cm long by 8 cm wide and could hold a maximum of 11 electrodes to make ten bipolar cell units. The electrodes were graphite, supplied by Ralph Coidan Ltd (Middlesborough), or IrO_2 coated Ebonex$^{\circledR}$ with dimensions 15 cm, 5 cm wide and 0.3 cm thick. The feeder electrodes were 0.6 cm thick. Ebonex$^{\circledR}$ is a magneli phase suboxide, (predominately Ti_4O_7) supplied by Atraverda Ltd. To hold the electrodes in place, weirs were grooved to the dimension of the interelectrode gap spacing (with grooves 0.3 cm deep). The electrolyte inlet weir was set at 2.0 cm (a total of 10 cm above the sieve plate) and the electrolyte outlet weir was set at 1.0 cm (a total of 9 cm above the sieve plate).

The reactor was operated as a set of bipolar cells, with electrical power supplied by a Farnell Instrument Ltd stabilized power d.c. supply situated outside the reaction module chamber. The SPER reactor module fits inside the main pilot plant tower reactor constructed of 10 cm internal diameter QVF glass. This reactor was located in a gas and electrolyte flow circuit as shown in Fig. 3.

The base of the column serves a dual purpose as the reservoir for the electrolyte and as the main reaction chamber. The electrolyte was pumped using a centrifugal pump, PI, (Totton Electrical Products, TEP, PC40/60) through two loops: the first was used to maintain the agitation of the electrolyte in the base of the SPER column and the second to form the bypass loop for the pump. In the second flow loop, the electrolyte was pumped through a heat exchanger, H2, and rotameter (GA Platon Ltd) to the bipolar reactor unit. When required the electrolyte was cooled or heated with water through the heat exchanger.

The ethene gas was supplied from a cylinder through a sequence of control valves to reduce the input pressure to the SPER to the operational level (approximately 1 bar). Ethene could be mixed with nitrogen

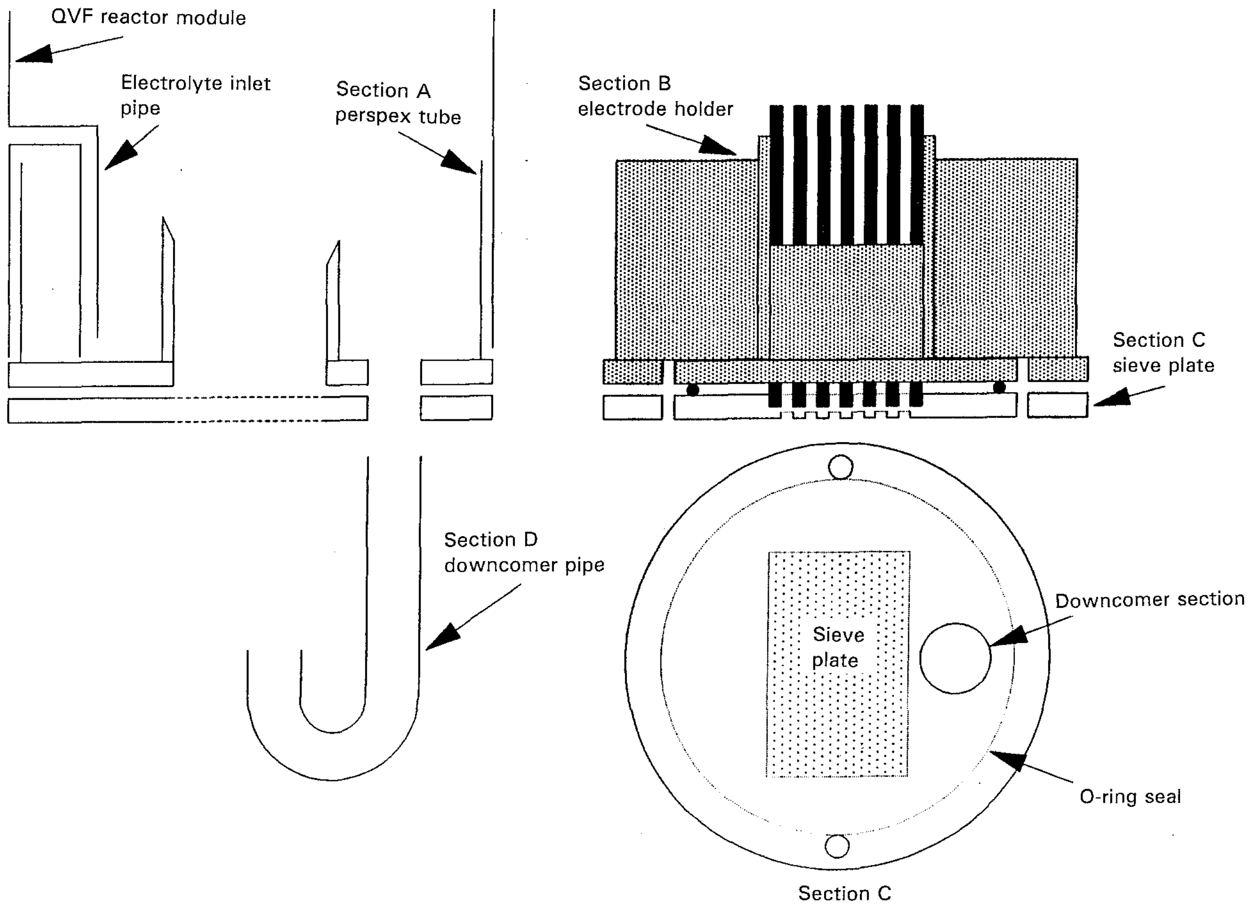

Fig. 2. SPER reaction unit.

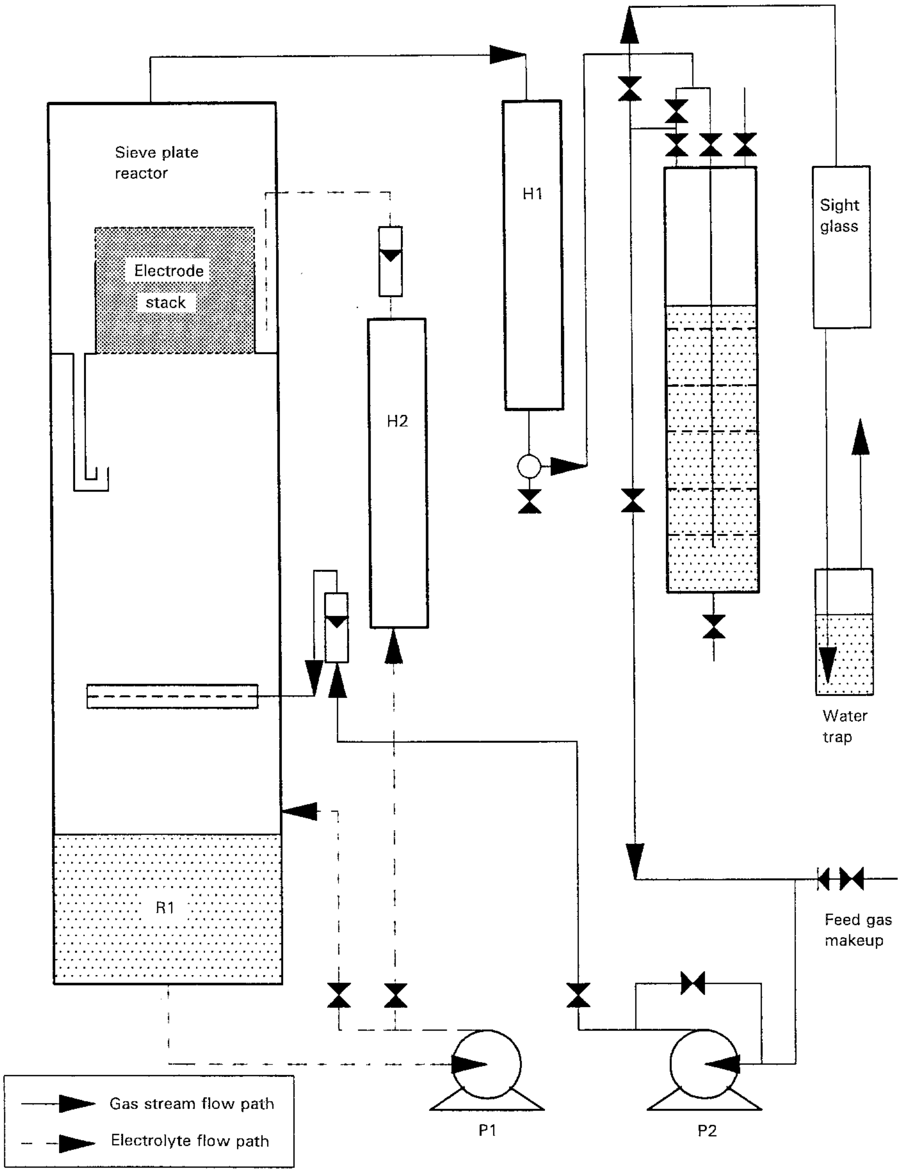

Fig. 3. Schematic flow diagram of the SPER unit.

to simulate the effects of the ethene concentration on the operation of the SPER to produce ethene oxide. For all experiments, the total flow rate of fresh feed gas entering the SPER was maintained at $60\,\mathrm{cm^3\,min^{-1}}$ (1 bar, 20 °C) and the electrolyte was always presaturated with ethene before the start of the trial. The inlet gas then joined the gas recycle line. The entire gas circuit was made of either stainless steel 316 or QVF glass. The gas was pumped through two loops. The first was for the bypass loop of the (Charles Austin B101DE) gas pump, P2. In the second loop, the gas was circulated upwards through a rotameter (R1) and into a QVF gas distributor on the SPER column. The gas then passed through the sieve plate and bipolar reactor, out at the top and into the heat exchanger, H1. From the heat exchanger, the gas passed into the ethene oxide removal column, where the ethene oxide carried by the gas was absorbed in either distilled water or sodium hydroxide electrolyte. The gas then divides between the purge section and the gas recycle line.

The electrolyte used in this work was $0.1\,\mathrm{kmol\,m^{-3}}$ KBr solution, unless otherwise stated. Temperatures of operation were varied between 11 °C and 40 °C. The electrolyte flowrate through the reactor was constant at $67\,\mathrm{cm^3\,s^{-1}}$ and the gas flowrate was $0.92\,\mathrm{dm^3\,s^{-1}}$ (1 bar, 20 °C) through the sieve plate. The operating pressure of the reactor was nominally 1 bar absolute. These conditions resulted in an electrode area of $50\,\mathrm{cm^2}$ exposed to electrolysis for each plate.

The concentrations of ethene, ethene oxide and other organic species in the SPER and in the absorber were analysed by gas–liquid chromatography (GLC) using stainless steel porapak Q column, with a Perkin-Elmer Sigma IB gas chromatography fitted with a flame ionisation detector. The inorganic byproducts, hypobromite and bromate were analysed by the standard thiosulphate method.

3. Experimental results and discussions

With the sieve plate reactor using bipolar electrodes the occurrence of current bypassing around the electrode may cause an increase in the system energy consumption. Current bypass manifests itself in an apparent loss in current efficiency for the full cell assemblies, in that the predicted faradaic yields of the full compliment of cells, all utilizing the main applied current density, is greater than actual faradaic yields. Current bypass can occur around the sides of the electrodes and beneath the sieve plate and is more significant for relatively small electrode area assemblies. Thus current inefficiencies discussed below do not always represent a loss of selectivity. Space time yields quoted in this work are based on the volume of the bipolar cell stack.

3.1. *Influence of sieve plate design*

An important factor in the performance of the unit is the absorption of ethene into the electrolyte. This was expected to be influenced by the sieve plate design and thus this factor was initially investigated. Two designs of sieve plates were used, with hole diameters of 1 mm or 2 mm, and details of the design parameters are given in Table 2. Generally the sieve plate design with the larger hole diameter and consequently lower number of holes resulted in an inferior current efficiency (see Table 3). This was presumably due to a poorer gas absorption and thus in subsequent tests the sieve plate with 1 mm hole diameter was used.

3.2. *Influence of temperature*

Figure 4 and Table 4 show the influence of temperature on ethene oxide production with the sieve plate design 2, with three bipolar cells. In all experiments the current efficiency decreased significantly with time and tended to approach a pseudo steady value. In the initial periods of the electrolysis, higher temperature of operation gave the higher current efficiencies. Most of the ethene oxide formed at 40 °C was found in the absorber of the plant (Fig. 4) and not the reactor. The concentration of ethene oxide in the reactor apparently approaches a steady–state value with the stripping of this species from the reactor by

Table 2. Sieve plate tray design parameters

Tray design	*Design 1 (SPD1)*			*Design 2 (SPD2)*	
Interelectrode gap/mm	3	9	15	6	24
Hole diameter/mm	1	1	1	2	2
Holes per bipolar cell	29	58	87	10	30
Electrodes	11	8	4	8	3
Bipolar cells	10	5	3	7	2
Interelectrode flow area/mm^2	138	414	690	300	1200
Hole area/mm^2	22.8	45.6	68.3	31.4	94.2
Hole ratio	0.17	0.11	0.10	0.10	0.08
Gas flow rate/dm^3 s^{-1}	0.92	0.92	0.92	0.92	0.92
Hole velocity/m s^{-1}	40.4	20.2	13.5	29.3	9.8

Table 3. Effect of SPER configuration on energy consumption and space time yield

Sieve tray design	*SPD1*	*SPD1*	*SPD1*	*SPD2*	*SPD2*
Space-time yield/kg h^{-1} m^{-3}	8.81	29.7	7.25	3.78	
Energy consumption/kWh kg^{-1} of ethene oxide	12.4	33.6	12.3	24.9	
Interelectrode gap/mm	9	9	15	24	24
Cells	5	5	3	2	2
Current density/A m^{-2}	202	680	206	200	600
Average bipolar stack voltage/V	30	72	20	20	
Temperature/°C	11	11	35	35	35
Ethene oxide current efficiency/%	60.9	44	68.7	54.2	30.3
Ethene oxide produced in 255 min/mmoles	155.4	530	127.9	77.3	127

Table 4. Effect of temperature on ethene oxide production for the SPER

SPER reaction cell temperature/°C	11	25	30	35	40
Bipolar stack voltage/V	31	24	21	21	18
No. of bipolar cells in stack	5	3	3	3	3
Current density/A m^{-2}	202	206	206	206	206
Ethene oxide current efficiency/%	44	53	55	59	54
Ethene oxide produced in 225 min/mmoles	155.4	115.3	118.7	127.9	116.5
Average energy consumption/kWh kg^{-1}	12.9	15.1	12.9	12.4	10.3
Space time yield/kg h^{-1} m^{-3}	8.8	6.5	6.7	7.2	6.6
Bromate current efficiency/%	2.2	0	–	0	0.3
Hypobromite current efficiency/%	9.1	0.6	–	5.8	0.8

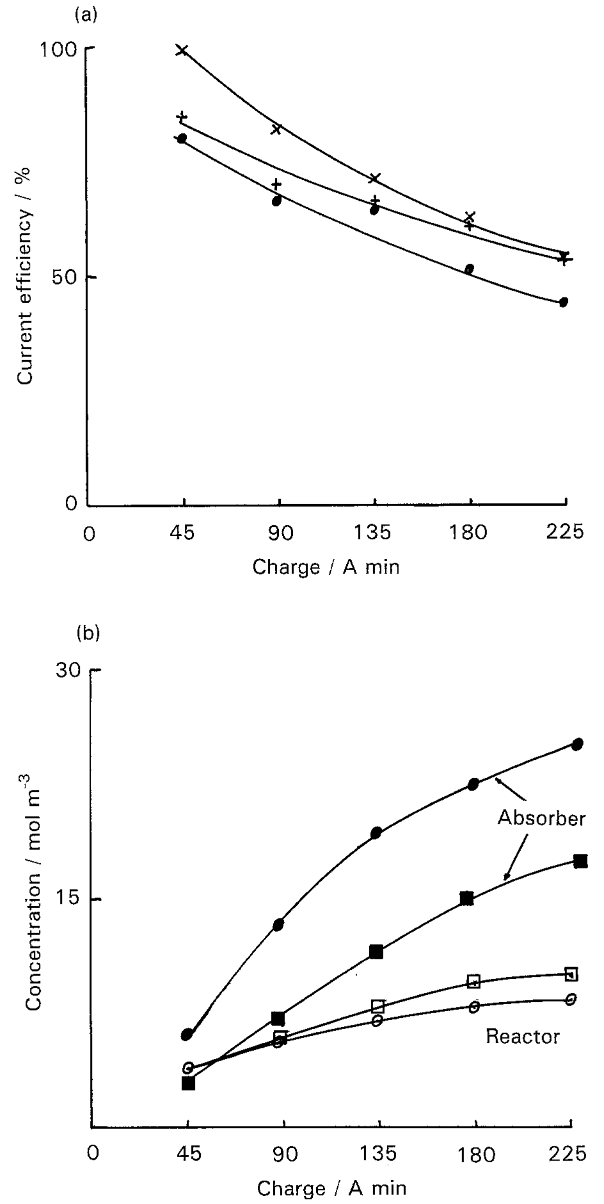

Fig. 4. Effect of temperature on the production of ethene oxide. (a) Variation of current efficiency with charge passed (×) 40 °C, (+) 25 °C, (●) 11 °C. (b) Variation of concentrations in the reactor and the absorber. Absorber: (●) 40 °C, (■) 25 °C; reactor: (○) 40 °C, (□) 25 °C.

gas flow a significant factor. As the ethene oxide concentration increases in solution with time a greater proportion will be in the gas recycle stream and thus more will exit with the gas-purge product stream. Thus an advantage of the higher temperature operation is the more efficient removal and phase separation of the product from the liquid into the gas phase. This serves to offset an increase in any rate of reaction of ethene oxide to ethene glycol by saponification. Clearly other chemical reactions may potentially increase at the higher temperature, although under the conditions used no other organic byproducts were detected and the formation of inorganic bromine species (bromate, hypobromite) was small, less than 2% current efficiency when three bipolar cells were used. With five cells and at a temperature of 11 °C, a significant amount of bromate and hypobromite was formed (Table 4). This was due probably to an increased rate of bromine generation in relation to the rate of ethene absorption. A significant disadvantage of operating at a temperature higher than 40 °C could be the reduced solubility of ethene.

An advantage of the higher temperature is the decrease in the energy consumption, from 15.1 kWh kg^{-1} at 25 °C to 10.3 kWh kg^{-1} at 40 °C due to a reduced cell voltage. The values of energy consumption are relatively high due to the high interelectrode gap (15 mm) used. In practice this gap can be reduced to lower the energy consumption.

3.3. *Effect of pH*

The effect of pH on the production of ethene oxide was investigated by introducing different standard buffer solutions. Figure 5 shows the variation of ethene oxide efficiencies at different values of initial pH, for a temperature of 11 °C and a current density of 204 A m^{-2}. Table 5 summarises conditions and data. The data indicate that there is significant benefit in the introduction of some control of pH. Both pH 6 and 10.1 buffers caused significant increases in the current efficiency. Over the duration of the runs, a value of pH of 6 apparently gave the best overall current efficiencies, although the initial current efficiencies showed a trend of increasing current efficiency from unbuffered to pH 6, 8 and 10.1 solutions.

The overall performance is, however, influenced by the variation in pH in both the reactor and absorber (Fig. 6) and the amount of ethene oxide present in both the reactor and absorber (Fig. 6(b)). It is noticeable that at a pH of 6, the majority of the ethene oxide remained in the reactor with little apparently being stripped into the absorber, thus accounting for the high current efficiencies, which are based on measured oxide concentrations in the absorber and the reactor solutions. The variation in pH had little effect on the formation of hypobromite and bromate, current efficiencies of bromate being less than 1%, and on the formation of any dibromoethene.

On comparing the variation of pH in the reactor

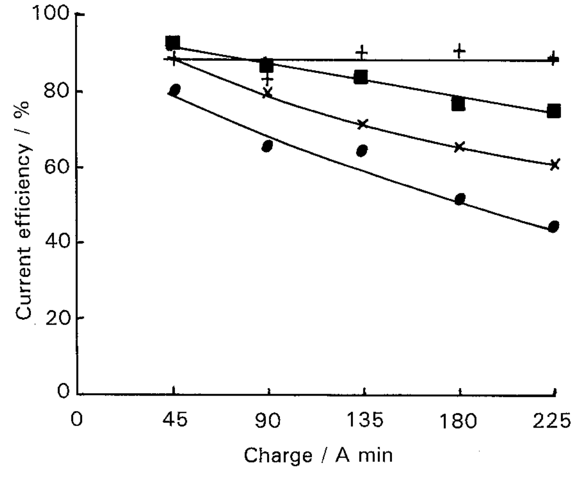

Fig. 5. Effect of pH on the current efficiency of ethene oxide formation. Conditions: 11 °C, 204 A m^{-2}. Key: (+) pH 6, (×) pH 8, (■) pH 10 and (●) unbuffered.

Table 5. Effect of pH on ethene oxide production

Buffer solution pH	*Unbuffered*	*6*	*8*	*10.1*
Bipolar stack voltage/V	31	29	28	23
Current density/A m^{-2}	202	204	206	206
Ethene oxide current efficiency/%	44	87.8	69	74.5
Ethene oxide produced in 225 min/mmoles	155.4	313.1	216	268.4
Energy consumption/kWh kg^{-1}	12.9	8.3	9.7	7.0
Space time yield/kg h^{-1} m^{-3}	8.8	17.7	12.2	15.2
Ethene oxide ratio (Reactor/absorber)	1.3	10.6	2.4	19.6

with the corresponding variation of current efficiencies it can be seen that the lowest current efficiencies occur with values of pH approaching 12, for the unbuffered operation, and with the use of pH 8.0 buffer. At values of pH of 10 or less, current efficiencies are generally high, greater than 75%. Control of pH, to a value of 10 or less appears to be important in giving high current efficiency. For a 0.1 kmol m^{-3} bromide ion solution this corresponds to a region of chemical equilibrium in which HOBr and Br_2 are significant. The increase in the value of pH in the absorber, confirms that both organic species and inorganic species, such as hydroxide (in water vapour) and bromine species, can be stripped out of solution.

The effect of pH on ethene oxide current efficiency at a higher current density of approximately 400 A m^{-2} was similar to that at 204 A m^{-2} as can be seen in Table 6. In this data different concentration of $NaHCO_3/Na_2CO_3$ buffer solution were used. The higher concentrations of buffer maintained reasonably constant values of pH, e.g. with 0.1 kmol m^{-3}, the pH increased by only 0.3. The higher current densities resulted in lower current efficiencies, partly due to increased bromate and hypobromite formation, but mainly due to increased current bypass, which is compounded by the increase in electrolyte conductivity due to addition of the buffer. With the higher concentrations of buffer the energy consumption is 11.6 kWh kg^{-1}.

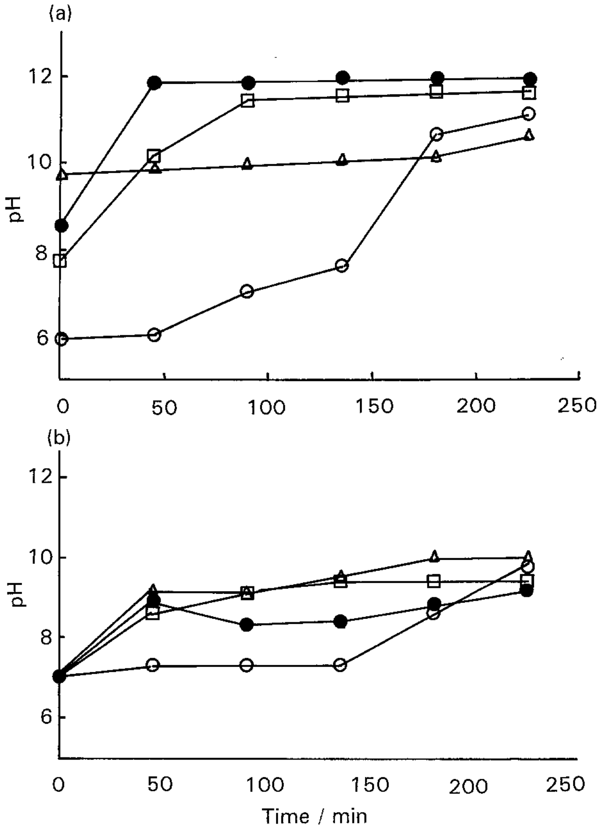

Fig. 6. Variation of pH with time in the reactor and the absorber. Conditions: 11 °C, 204 A m^{-2}. Key: (○) pH 6, (□) pH 8, (△) pH 10 and (●) unbuffered. (a) Reactor and (b) absorber.

3.4. *Effect of electrode material*

Graphite is not the ideal bipolar electrode material for this work as it undergoes slight corrosion and erosion over relatively short operating times and has a relatively high overpotential for bromine evolution. An alternative anode material used in this work was iridium oxide coated ebonex®. Ebonex is a magneli phase titanium suboxide, primarily Ti_4O_7 and Ti_5O_9, which is electrochemically conducting and electrochemically stable. Only limited amounts of this material were available, sufficient to form two bipolar cells, using Ebonex coated on one side only, with IrO_2 as a central bipolar electrode and an anode feeder. The sieve plate design used 2 mm diameter holes (SPD2). Table 7 compares the performance with that of an equivalent design using graphite electrodes and the results are quite similar. The use of IrO_2 oxide coated Ebonex® did not affect the amount of hypobromous acid or bromate formed in this work. Thus further developments of this epoxidation process could be pursued using coated Ebonex® materials.

4. Conclusions

The positive results from the SPER design in the oxidation of ethene are as follows:

(i) The extent of current bypass is relatively small at low current densities as indicated by initial current efficiencies approaching 100%. At higher current densities the amount of current bypass increases, which has a major effect of increasing the energy consumption.

(ii) The formation of byproducts is relatively small with only a small percentage of the current leading to bromate and hypobromous acid formation. The formation of organic byproducts, notably dibromoethene, is negligible as a result of the low concentration of bromide ion used, selected on the basis of minimizing this organic byproduct. Equivalent runs with a higher concentration, 0.2 kmol m^{-3} of potassium bromide, realized relatively high concentrations of dibromoethene, equivalent to a 7.5% current efficiency at a current density of $300\,\mathrm{A\,m^{-2}}$. This not only reduces selectivity and complicates product separation, but is a major loss of the relatively expensive bromide electrolyte.

A major factor in the design of the sieve plate electrochemical reactor is that the product gas stream consists of a mixture of ethene (with oxide) diluted by hydrogen formed at the cathode and oxygen formed at the anode. The greater the conversion of ethene to ethene oxide which is achieved, the lower is the concentration in the liquid electrolyte due to the lower partial pressure of ethene. Thus, at least with a single stage reactor, a reduced rate of ethene oxide production occurs corresponding to a lowering in current efficiency and an increase in energy consumption. A high ethene conversion is desirable due to the high costs of separation of ethene/hydrogen mixtures. The greatest overall conversion of ethene achieved in this work was 87% at a current density of $680\,\mathrm{A\,m^{-2}}$ although current efficiency for ethene oxide production was low, less than 45%, and the formation of bromate and hypobromite were high at 5.2% and 4.0% current efficiency, respectively. This apparently limits the applicability of the SPER as a single stage unit. However the eventual application of a SPER is as a multistage counter-current gas/liquid contactor and in this mode of operation higher conversions of ethene can be anticipated.

References

[1] J. A. M. Leduc (to M. W. Kellog Co.), *British Patent 1 064 961* (1967).

[2] M. Fleischmann, R. E. W. Jansson and K. Ashworth, *British Patent 1 504 690* (1978).

[3] P. Robertson, P. Cettou, D. Matic, F. Schwager, A. Stork and N. Ibl, *AIChE Symp. Ser. no.* **185** (1979) 115.

[4] M. Fleischmann, J. W. Oldfield and C. L. K. Tennakoon, *IChemE Symp. Ser. no.* **37** (1973) 1, 53.

[5] S. Ehdaie, PhD thesis, Southampton University, UK (1979).

[6] K. G. Ellis and R. E. W. Jannson, *Chem. Ind.* (*London*) (1980) 864.

[7] S. Harrison, PhD thesis, University of Newcastle upon Tyne, UK (1986).

[8] K. Scoffham, PhD thesis, University of Newcastle upon Tyne, UK (1979).

[9] Kroening and Konrad (Farbenfabriken Bayer AG), *German Patents 1 252 649* (1967) *1 258 856* (1968), *1 258 857* (1968); *French Patents 1 540 800* (1968), *1 570 279* (1968), *1 575 783* (1968), *2 008 178* (1980).

[10] K. H. Simmrock, *German Patent 2 658 189* (1978).

[11] F. Beck and J. Heiss, *German Patent 2 336 288* (1975).

[12] K. Scott, C. Odouza and W. Hui, *Chem. Eng. Sci.* **47** (1992) pp 2957–2962.

[13] A. Manji and C. W. Oloman, *J. App. Electrochem.* **17** (1987) 532.

[14] K. Scott and W. Hui, *Chem. Eng. J.*, to be published.